Selectivity of Bio-oils Catalytic Hydrotreatment Assessed by Petroleomic and GC*GC/MS-FID Analysis

ARTICLE *in* ENERGY & FUELS · MARCH 2013

Impact Factor: 2.79 · DOI: 10.1021/ef302145g

4 AUTHORS, INCLUDING:

Vincent Carre
University of Lorraine
23 PUBLICATIONS **187** CITATIONS
SEE PROFILE

Frederic Aubriet
University of Lorraine
46 PUBLICATIONS **491** CITATIONS
SEE PROFILE

Anthony Dufour
French National Centre for Scientific Research
58 PUBLICATIONS **745** CITATIONS
SEE PROFILE

energy&fuels

Article

pubs.acs.org/EF

Selectivity of Bio-oils Catalytic Hydrotreatment Assessed by Petroleomic and GC*GC/MS-FID Analysis

Roberto Olcese,[†] Vincent Carré,[‡] Frédéric Aubriet,[‡] and Anthony Dufour*[,†]

[†]Reactions and Processes Engineering Laboratory, CNRS, Lorraine University, ENSIC, 1 rue Grandville, 54000 Nancy, France

[‡]Laboratoire Chimie et de Physique des Milieux Complexes, Lorraine University, ICPM, 1 Boulevard Arago, 57078 Metz, France

Supporting Information

ABSTRACT: We propose to assess the selectivity of hydrotreatment catalysts by two complementary analytical methods: (1) high-resolution mass spectrometry (MS), called "petroleomic" analysis, by Fourier transform ion cyclotron resonance (FT ICR, 9.4T) MS for species heavier than m/z of about 200 Da and (2) quantitative GC*GC (heart-cutting)/MS-flame ionization detector (FID) analysis of lighter species. The methodology is illustrated on methanol-soluble bio-oils produced by lignin pyrolysis and hydrotreated by iron-based catalysts. GC*GC analysis is calibrated by a combination of internal standard and prediction of response factors on the FID. Laser desorption ionization (LDI) and electro spray ionization (ESI) in negative-ion mode are combined for the petroleomic analysis. The selectivity of hydrotreatment (catalytic fixed bed, 1 atm, 400 °C) is assessed as a function of catalyst loads and iron support (silica and activated carbon). Hundreds of species are analyzed by GC*GC and petroleomic and mapped in Van Krevelen diagrams. The high selectivity of reduced iron for the hydrodeoxygenation of lignin pyrolysis vapors is demonstrated. The effect of the catalytic treatment on oxygen content and unsaturation is studied for a broad range of species: from C_2 to C_{14} by GC analysis and from C_8 to C_{37} by petroleomic. Many heavy lignin oligomers produced by the pyrolysis are trapped by the catalytic bed, highlighting the need of new catalytic systems to convert them into valuable fuels or chemicals.

1. INTRODUCTION

The thermo-chemical conversion of lignin-cellulosic biomass is an attractive route for chemicals and biofuels productions. Pyrolysis and liquefaction are promising routes to produce liquid intermediates ("bio-oils") for biofuels and added value chemicals (such as aromatics) because current refinery infrastructures could be used and adapted to upgrade the bio-oils, without large capital investments for new reaction equipment.[1] Moreover, the local production of intermediate bio-oils (with a much higher energy density than the original biomass) could reduce biomass transport issues and promote a local processing of biomass.

The main hurdle to overcome for fast pyrolysis is the high oxygen content in bio-oils, leading to oil stability and to corrosion problems and the huge amount of different species produced (selectivity issues).[2] The main strategies for bio-oil deoxygenation are cracking over zeolites[3] or hydrodeoxygenation (HDO).[4]

Bio-oil is a very complex mixture of hundreds of chemical species that can be classified as water (~25% mass), volatiles (analyzed by gas chromatrography (GC), 35% mass), non volatile (analyzed by liquid chromatography (LC), 15%), and water-insoluble compounds (pyrolytic lignin, ~25%).[5] Many methods were proposed for bio-oils fractionation[6,7] and analysis: size exclusion chromatrography (SEC),[8,9] GC/mass spectrometry (MS),[10−12] field ionization MS,[13] laser desorption MS,[13] low energy electron impact MS,[14] small-angle neutron scattering,[15] nuclear magnetic resonance,[8,16,17] Fourier transform infrared spectroscopy,[8] etc.

Nevertheless, there is still a strong need for analytical strategies able to depict a broad "chemical signature" of bio-oils especially as a function of catalytic up-grading conditions. Such a "chemical signature" could be assessed by the "petroleomic" method.

The petrolomic methodology has been introduced by Marshall[18,19] and extensively used for crude oil,[20−23] diesel fuel,[24] coal liquefaction oil,[25] and recently was applied to bio-oils from biomass pyrolysis.[26−30] The high mass measurement accuracy (100−400 ppb) and resolution ($m/\Delta m_{50\%} > 100\,000$) of the mass spectrometers (such as Fourier transform ion cyclotron resonance MS, FT ICR MS) enable one to resolve thousands of peaks in complex mixtures at the level of molecular formula assignment.[18] These species are mapped as a function of their relative abundance, for instance, in the Van Krevelen diagram.

To our knowledge, Smith et al.[26] conducted the first petroleomic study on pyrolysis bio-oils using laser desorption ionization (LDI) linear ion trap-orbitrap MS. Three high-resolution mass spectrometers were then compared by this group using electrospray ionization (ESI) in negative ion-mode.[27] Among many findings, Smith et al.[27] showed the effect of pH on the relative ion abundance of some major peaks (including phenolics from lignin pyrolysis).

Jarvis et al.[28] compared the composition of oily and aqueous phases of pine and peanuts derived bio-oils by negative ESI FT ICR MS. They identified more than 10 000 peaks and demonstrated the unique ability of ultra high-resolution FT ICR MS to identify elemental compositions of bio-oils. Liu et

Received: December 22, 2012
Revised: March 5, 2013
Published: March 5, 2013

   dx.doi.org/10.1021/ef302145g | Energy Fuels 2013, 27, 2135−2145

al.[29] studied by negative ESI FT ICR MS the composition of bio-oils subfractions soluble in hexane, dichloromethane, methanol, or ether. FT ICR MS has been also used on lignin model compounds[30] and on lignin hydrothermal products.[31]

Petroleomic is a very powerful method, but it gives only the relative abundance of species (relative to all analyzed species). Other methods are needed to assess the quantitative yields in goal products relative to the initial biomass weight.

FT ICR MS was combined with GC/MS to investigate pine bio-oils,[29] NMR to study lignin hydrothermal selectivity[31] and the composition of different organic matters,[32,33] and comprehensive GC*GC on vacuum gas oils.[34]

Comprehensive GC*GC methods have been tailored for bio-oils catalytic up-grading[35] but not yet combined with petroleomic on bio-oils.

The selectivity of catalytic treatments has been assessed by petrolemic method for hydrotreated diesel fuel[36] or oil,[37] gas oil,[38] hydrocracking over zeolite,[39] and coal liquefaction.[40] To date, only Jarvis et al.[41] have used the petroleomic approach to assess the catalytic conversion of bio-oils over zeolite (HZSM-5).

To the best of our knowledge, we provide the first study using FT ICR MS analysis combined with GC*GC (heart-cutting) analysis to assess the selectivity of bio-oils catalytic conversion. These powerful and complementary methods are illustrated on lignin methanol-soluble products hydrotreated over iron-based catalysts. The selectivity in HDO is compared for two catalyst loads and two types of support (iron over silica or activated carbon). Ionization by laser desorption (LDI) and electro spray (ESI) are compared and combined for petroleomic. Concerning heart-cutting GC*GC/MS-FID analysis, a quantitative method based on a combination of internal standard calibration and FID response factor predictions is proposed. This analytical work highlights some issues on catalytic reactors engineering for hydrotreating biomass pyrolysis vapors.

2. MATERIALS AND METHODS

We chose to develop the gas-phase hydrotreatment of pyrolysis vapors over cheap catalysts (iron-based),[42,43] instead of the liquid-phase hydrotreatment of bio-oils. Indeed, this route could reduce the problem of handling the reactive lignin oils and promote heat recovery. Moreover, the hydrogen partial pressure could be low (0.3 bar, typical of a syngas),[42] and separating pyrolysis and catalytic reactors offers a more versatile process (different temperatures, regeneration cycles, etc.).

2.1. Catalysts' Preparation and Properties. Iron over silica (Fe/SiO_2) catalyst was prepared by simple impregnation. 15.65 g of silica (Aerolyst 3039, Degussa; grounded and sieved 100−380 μm) was contacted with a solution of 20.15 g of iron nitrate nonahydrate (Sigma) in 46 mL of deionized water. The mixture was exposed to vacuum at room temperature for 3 h, and then dried 24 h at 100 °C. The resulting impregnated solid was regrounded and sieved (100−380 μm), and then treated under argon flow (50 N mL/min) with temperature increasing from 25 to 500 °C at 5 K/min and held at 500 °C for 1 h, then cooled to room temperature under argon flow. Gas flow was switched to 50 N mL/min of H_2, and temperature was reraised to 500 °C at 5 K/min and held during 1 h. The catalyst then was cooled to room temperature and passivated at room temperature using a gas with 100 ppm of O_2 in argon. Iron over activated carbon catalyst (Fe/AC) was prepared by the impregnation of 14 g of activated carbon NORIT RX-3 "Extra" (100−380 μm) with a solution of 11.24 g of iron nitrate and 14 mL of water. It was treated afterwards as Fe/SiO_2 catalyst.

Before catalytic experiments, the catalysts were reduced in situ under 300 N mL/min of H_2, increasing temperature at 5 K/min until reaching reaction temperature (400 °C). For more details about preparation and characterization, see refs 42, 43. Chemical analysis of the catalysts (by Mössbauer, XRD, etc.) is out of the scope of this Article.[42,43]

The main characteristics of the catalysts are summarized in Table 1.

Table 1. Main Characteristics of the Catalysts[43]

sample name	support	iron load (wt %)[a]	iron crystallite size (nm)[b]	BET surface area (m^2/g)[c]
Fe/SiO_2	silica (Aerolyst 3039, Degussa)	14.7	17	130
Fe/AC	activated carbon (Norit RX-3)	11.1	20	1200

[a]Analyzed by ICP/MS, calculated for reduced iron. [b]By XRD analysis based on Scherrer's equation at $2\theta = 44.6°$ ($K = 0.9$). [c]Analyzed by N_2 sorption after iron impregnation and calcination under argon.

2.2. Pyrolysis of Lignin, Direct Catalytic Hydrotreatment of Pyrolysis Vapors in a Fixed Bed Reactor, and Sampling of Products. Organocell lignin was supplied by the Institute of Wood Chemistry (Hamburg, Germany). Lignin and char were analyzed with a Thermo Scientific Flash Elemental Analyzer CHNS. Oxygen mass percentage was determined by difference.

Lignin pyrolysis and catalytic conversion of the vapors were conducted in a lab-scale setup presented in the Supporting Information. It is a simple tubular pyrolysis reactor coupled to a fixed bed reactor for catalytic hydrotreatment of vapors. The design is suited for a good control of pyrolysis and catalytic conditions and to reduce cold zone in transfer lines from pyrolysis to products sampling. Its purpose is not to maximize liquid products from lignin but rather to investigate the composition of hydrotreated products from a real lignin stream by a simple procedure. The setup consists of a steel tubular reactor preheated at 500 °C (thermocouple in the pyrolysis zone) continuously swept by 300 N mL/min of N_2 (analytical purity). Lignin (475 mg, anhydrous basis) was quickly introduced into the preheated furnace by a steel sample boat. The pyrolysis was almost completed after about 4 min of solid (lignin then char) residence time in the preheated reactor. The carrier gas flow rate was maintained during 10 min. The reactor was thus purged during 6 min after the apparent end of the pyrolysis. A fixed-bed reactor was directly connected to the outlet of the pyrolysis reactor. The catalytic reactor is a 10 mm internal diameter steel pipe externally heated to 400 °C (thermocouple inside the catalytic bed). 300 N mL/min of H_2 (Air Liquide, analytical purity) was introduced at the inlet of the fixed bed and mixed with the pyrolysis vapors. Catalyst was packed by means of quartz wool plugs. The catalyst load was 2 or 4 g. It is meaningless to regard the ratio of catalyst load over lignin mass on this setup because the catalyst should be tested on a continuous pyrolysis reactor with long time on stream experiments and regeneration cycles. Moreover, the iron-based catalysts are much cheaper and less hazardous than other ones previously proposed in the literature.[43]

The exit of the catalytic reactor was connected to two impingers (both with frits) filled with 10 mL of methanol to sample condensable vapors. The connection line was reduced to its minimum (few centimeters at ∼350 °C) and rinsed after each experiment. The first impinger was cooled at 0 °C (ice) and the second one at −60 °C (by 2-propanol mixed with liquid N_2). Once the pyrolysis was finished, both impingers were washed (including connection lines) with about 5 mL of methanol. One microliter of 1-undecene was added in each impinger as internal standard for GC. A negligible amount of products was always analyzed in the second impinger, demonstrating the suitability of the sampling train.[44] Methanol was chosen as the best solvent to dissolve even heavy fractions from lignin pyrolysis.[7,13,28,29] Moreover, it is a good solvent for the ionization of lignin oligomers with negative-mode ESI.[45] The solutions from the impingers were analyzed by GC and FT ICR MS analysis without any other preparation (nor dilution). To sum, bio-oils produced from 475 mg of

lignin were diluted in about 15 mL of methanol (10 mL of methanol in the first impinger + 5 mL for rinsing impinger and connection lines). The concentration range for the sum of all GC-oils was around 2 mg/mL and for individual species (such as phenol) around 10 μg/mL. It remains impossible to estimate the concentration in the products analyzed by FT ICR MS.

2.3. GC*GC (Heart-Cutting)/MS-FID-FID Analysis. Light products (called hereafter "GC-oils") were analyzed with an Agilent 7890 gas chromatographer coupled to an Agilent 5975C MS analyzer. One microliter of the methanol solution recovered from impingers (with products and internal standard) was injected with a split ratio of 20 into an Agilent HP-5MS (diphenyl 5%, dimethylpolysiloxan 95%, 30 m × 250 μm × 0.25 μm) column (0.93 N mL/min of He) connected with a heart-cutting system to an Agilent DB-Wax (polyethylenglycol, 30 m × 320 μm × 0.25 μm) column (3.44 N mL/min of He, heart-cutting time: 26−27.3 min). These two columns were chosen for GC*GC because they exhibit complementary polarities and high separation power. The oven temperature program was: 40 °C (hold 10 min), then increased at 5 K/min to 200 °C (hold 21 min). The exit of HP-5MS was connected simultaneously to a FID and to the MS (see Figure 1). The exit of DB-Wax column was connected to a separate FID.

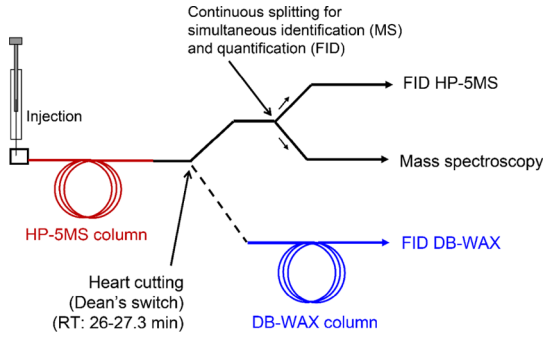

Figure 1. Scheme of the GC*GC (heart-cutting)/MS-FID-FID device (2 columns and Dean's switch valve) used for identification and quantification of products of lignin pyrolysis and catalytic hydrotreatment.

A typical chromatogram is presented in Figure 2.

A list of identified compounds with retention times and elemental formulas are given in the Supporting Information. More than 170 different compounds were detected and qualified by MS and NIST database (see the Supporting Information). Between 70 and 93 compounds were quantified depending on the experimental conditions.

A combination between experimental calibration by internal standard (1-undecene) and FID response factors prediction was used. The complete calibration procedure is presented in the Supporting Information. This method allows quantifying up to hundred of compounds by a single injection, with a limited (time-saving) calibration. Briefly, the response factor on FID was determined experimentally for 11 key lignin products relative to 1-undecene (internal standard) with three standard solutions. The response factors on FID of other compounds were predicted using the method of de Saint Laumer et al.[46] (see the Supporting Information).

2.4. Petroleomic Method by High-Resolution FT ICR MS Analysis: Negative-Ion Mode Laser Desorption Ionization (LDI) and Electro Spray Ionization (ESI). *a. Fourier Transform Ion Cyclotron Resonance Mass Spectrometer.* The used Fourier transform ion cyclotron resonance mass spectrometer (IonSpec, Lake Forest, CA) is equipped with an actively shielded 9.4-T superconducting magnet (Cryomagnetics, Oak Ridge, TN). Two different and independent devices including an external ion source, a pumping system, an ion transfer line, and an ICR cell were used. The first one for LDI−MS measurement is the so-called ProMaldi card, and

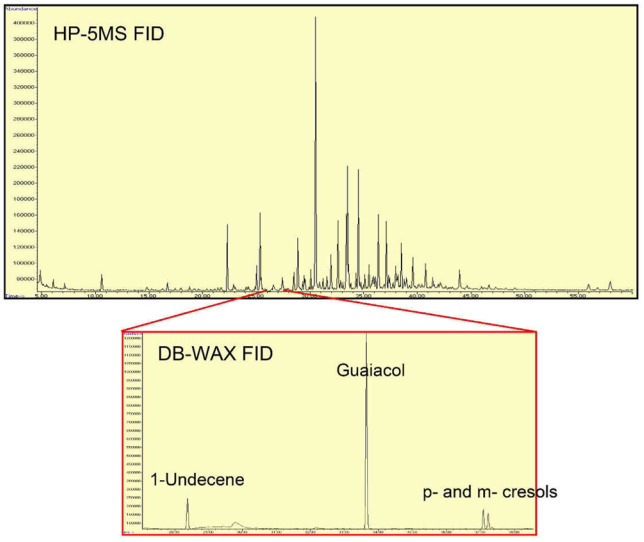

Figure 2. Chromatograms (FID signal) of lignin pyrolysis (no catalyst in the second reactor at 400 °C) on HP5 and DB-wax columns highlighting the heart-cut zone on HP5 column injected into the DB-Wax column. 1-Undecene is the internal standard. The chromatograms for 4 g of Fe/SiO_2 experiment are given in the Supporting Information.

the second one, the ESI card, is fitted with a Micromass Z-spray electrospray source.

b. Ionization Methods. For ESI FT ICR MS analysis, solutions were infused at a flow rate of 2 μL/min in the ionization source, which was at a temperature of 120 °C. The needle of the probe was set at 4.3 kV. The potential of the extraction skimmer and the skimmer at the entrance of the mass spectrometer were kept at −45 and −10 V, respectively. Nitrogen was used as nebulization gas. The nebulization and extraction conditions were adjusted to prevent fragmentation of the produced ions by the so-called in-source activation processes. After extraction, ions were stored in a hexapole for 2 s prior to be transferred into the ICR cell.

For LDI FT ICR MS experiments, some drops of the solutions (the same as for GC and ESI analysis) were deposited on a stainless steel holder. After evaporation of the solvent, the holder is introduced in the source of the mass spectrometer. The ions generated by 8 laser shots on the sample at a 355 nm wavelength (Nd:YAG, Orion, 5 ns time duration, spot area close to 0.056 mm^2, 250 mJ/cm^2) were first extracted from the ionization source and stored in a hexapole before being transferred into the ICR cell. To prevent fragmentation and to allow the ions to be efficiently stored in the hexapole, the ions were cooled by pulses of nitrogen gas. The used laser power is higher than the power used by Smith et al.[26] Nevertheless, the quick cooling by N_2 gas allows one to de-excite efficiently the generated ions.

c. Mass Spectrometric Data Acquisition and Analysis. The transfer of the ions from the storage hexapole to the ICR cell was conducted by a hexapole in RF-only mode. This mode limits time-of-flight effect and discrimination.[47] Nevertheless, a low and a high mass cutoff does exist. In our case, it was chosen to efficiently transfer species in the 200−600 m/z range. By increasing or decreasing the amplitude of the RF to investigate species with higher or lower m/z value, a dramatic decrease of abundance was observed between 200 and 600 without a significant modification in the low or high m/z range.

After their transfer in the FT ICR cell, ions are first thermalized by a pulse of nitrogen gas, before being excited by the application of appropriate RF, the frequencies of which correspond to the frequency of ions gyration in the 150−1000 m/z range, when they are submitted to a 9.4-T magnetic field. The radius of their trajectory is increased to be close to the receipt plates on which they induce a current. The detection of this current, the use of fast Fourier transform algorithm,

dx.doi.org/10.1021/ef302145g | Energy Fuels 2013, 27, 2135−2145

and the application of the relationship between the measured frequency and the m/z ratio give the mass spectrum. Mass spectra were acquired during 2 (or 1) seconds with 4 MW transient size. A mass resolution close to 600 000 (or 300 000) is obtained at m/z 200. To increase the signal/noise ratio, 5−20 mass spectra are accumulated. More spectra were not coadded by LDI for different reasons. First, the purpose of this study is to compare the chemical composition of the samples on peaks with a significant signal/noise ratio to depict the general trends associated with the catalytic hydrotreatment. An increase of S/N by a factor 4 is suitable for an efficient comparison of the samples. Second, it was also difficult to coadd more mass spectra during LDI−MS experiments. Indeed, the size of the sample deposit did not allow more than 20 mass spectra to be acquired on the same spot. Finally, it has also to be kept in mind that ions produced by LDI have to be thermalized before being transferred into the ICR cell. It requires introducing nitrogen gas during ion storage into the ion source. Nitrogen consumption should be limited to maintain a constant pressure in the nitrogen tank (80 Torr) and to keep constant the thermalization conditions between each mass spectra.

After the acquisition, the mass spectrum is internally recalibrated according to some peaks, which have been unambiguously identified. These peaks are relative to $C_xH_yO_4^-$ ions and are in the 217−475 m/z range. Elemental composition of each detected signal with a signal-to-noise ratio higher than 3 was determined by using the Composer device (Sierra) with the following search criteria: $C_{6-100}{}^{13}C_{0-2}H_{6-100}N_{0-2}O_{0-20}S_{0-1}$ general formula and a 2 ppm tolerance error. For the m/z < 500 ions, mass resolution was sufficient enough (>150 000) to distinguish ^{12}CH from ^{13}C, which only differ by 0.00448 Da.

3. RESULTS

3.1. Mass Balance. The GC-analyzed products of lignin pyrolysis without catalyst in the hydrotreatment reactor (at 400 °C) represented 8.7−9.5% wt of initial dry lignin. This result is consistent with the literature.[48] When a catalyst is used, the mass yield in GC-analyzed oils decreases. Mass yield of GC-analyzed oils was 5.7−6.1 wt % for catalytic runs. The decrease in GC-oils yields can be explained by HDO reaction that removes O atoms to replace them with H (and producing mainly water, which was not analyzed), by methoxy groups that are cleaved on the $C_{aromatic}$−OMe bond to form methanol (not analyzable with methanol as the solvent), or by conversion of GC-oils into carbonaceous species that deposit on the catalyst surface. The investigation of carbonaceous deposit is out of the scope of this Article.

The mass yield in substituted monoaromatic (6 wt %) is lower than for lignin hydrothermal conversion[31] due to the carbon converted in char (42 wt %) during pyrolysis instead of bio-oils. Yet the conversion time is 10 times lower, and operating conditions are more convenient (atmospheric pressure) for pyrolysis.

The relatively low mass yield in GC analyzable products emphasizes the need of other methods (such as petroleomic) to assess products composition and catalysts selectivity.

3.2. Distribution of Species Quantified by Heart-Cutting GC*GC in the Van Krevelen Diagram. The hundreds of species quantified by GC*GC method are listed in the Supporting Information with their elemental formula. The overall atomic O/C and H/C ratios presented in Figure 3 are based on the weight fractions of all quantified products and their respective elemental formulas. All Van Krevelen diagrams presented in this Article are rather "modified" Van Krevelen diagrams because O/C is plotted as a function of H/C. O/C is usually on the x-axis in Van Krevelen diagrams.[49]

The average O/C decreases during the HDO of pyrolysis GC-oils (from 0.248 to 0.094 for 4 g of Fe/SiO_2, Figure 3), but

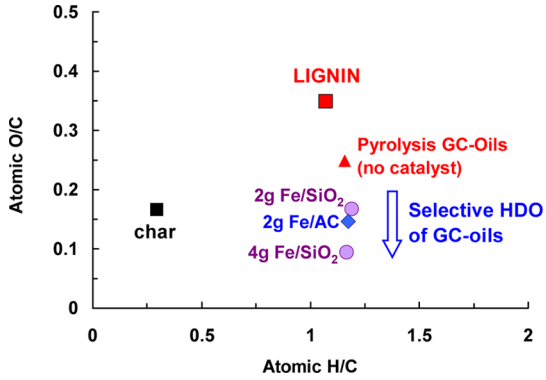

Figure 3. Van Krevelen diagram of lignin, char (based on elementary analysis), and GC-analyzed oils (based on GC*GC advanced quantification) obtained from HDO of lignin pyrolysis vapors on iron-based catalysts. A very selective HDO is revealed: O/C atomic ratio is reduced without affecting H/C ratio.

the H/C ratio is not markedly affected by the catalytic treatment. H/C ratios are 1.16 and 1.17 for pyrolysis without catalyst and 4 g of Fe/SiO_2 experiments, respectively.

The iron-based catalysts are selective for the HDO of lignin derived vapors because they catalyze the hydrogenation of the $C_{aromatic}$−O bond but not the hydrogenation of the aromatic rings (increase in H/C) and with minor cracking or growth (decrease in H/C) of GC-oils. Indeed, very few PAHs and no hydrogenated ring products were analyzed by GC/MS. We previously explained the reasons of this high selectivity based on the mechanisms of guaiacol HDO.[42,43]

The overall atomic ratio does depict the global selectivity of the hydrotreatment but not the high diversity of the compounds. Indeed, each point depicted in Figure 3 accounts for the contribution of tens of GC-analyzed species. These respective contributions are presented in Figure 4. One compound is represented by one circle with the area proportional to its weight fraction. The contributions in oxygenated aromatics (with two or more oxygen atoms per aromatic ring such as guaiacol, catechol, vanillin, etc.), phenols, or deoxygenated aromatics are highlighted as a function of the catalytic conditions. Concentric circles represent isomers.

The chemical composition of the lignin pyrolysis (without catalyst) is in agreement with other studies.[48] This experiment was conducted with the empty catalytic reactor set at 400 °C (as for catalytic experiments) and a mean residence time of the gas phase of around 0.3 s. Secondary reactions could thus occur. The aim of this experiment was not to study the chemical composition of purely primary pyrolysis products but rather to investigate the effect of the catalysts on lignin products.

The improvement of the lignin-derived bio-oil quality by the catalytic treatments is well displayed by the Van Krevelen diagrams. Fe/SiO_2 catalyzes the formation of benzene, phenol, and other useful products at the expense of unstable molecules with two or more oxygen atoms per aromatic ring (such as guaiacol, catechol, vanillin, etc.). Benzene and alkyl-benzenes are produced. Some of them could be refined for commercialization (p-xylene), but the mixture of aromatic hydrocarbons could also be a good biobased blend for fuels.[50]

2 g of Fe/SiO_2 and 2 g of Fe/AC led to the same overall atomic ratio of GC-oils (Figure 3) but to very different molecular selectivity displayed in Figure 4b and d. An important effect of the support (silica or activated carbon) is

dx.doi.org/10.1021/ef302145g | Energy Fuels 2013, 27, 2135−2145

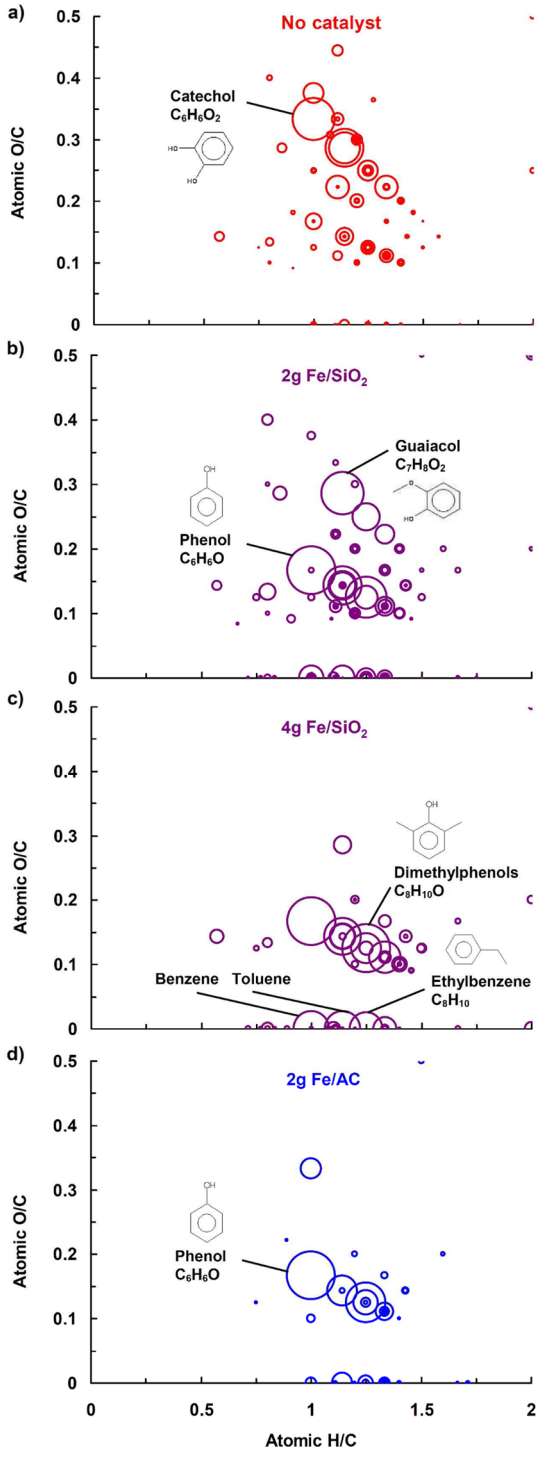

Figure 4. Distribution in all species quantified by GC in Van Krevelen diagram for (a) lignin products without catalytic treatment (empty second reactor at 400 °C), (b) 2 g of Fe/SiO_2, (c) 4 g of Fe/SiO_2, and (d) 2 g of Fe/AC. Pyrolysis and fixed bed reactors set at 500 and 400 °C, respectively, for all conditions. One circle depicts one molecular compound. The area of each circle is a function of the weight yield of each corresponding molecule.

evidenced in agreement with our previous study on guaiacol HDO.[43] Fe/AC leads to a lower diversity in products with a high selectivity in phenol (1.25 wt % phenol/dry lignin) and a very low selectivity in deoxygenated aromatics (such as benzene). This different selectivity between AC and SiO_2 can be explained by different surface moieties affecting phenols/support interactions.[43,51]

An interesting feature of the iron-based catalysts is their ability to preserve the aromatic rings and also to promote alkylation. The progressive increase in the H/C ratio from lignin oils to 2 and 4 g of Fe/SiO_2 experiments can be observed for O/C of 0.125, which corresponds to dimethylphenols (Figure 4 c). Ethylbenzene is also formed (Figure 4 d). This increase in H/C is offset in the overall H/C ratio, presented in Figure 3, by phenol and benzene formation. Alkylation could result from the pool of methyl species at the surface of the catalysts, such as methanol and radicals. More fundamental studies are needed to elucidate this mechanism on the complex lignin vapors.

3.3. Petroleomic Analysis by FT ICR MS. To date, the selectivity of bio-oils catalytic treatment has been mainly assessed by GC analysis and so only for light species (m/z lower than about 250 in our case). We propose to combine GC analysis with petroleomic analysis to investigate the selectivity for heavier species (m/z higher than about 200) as well.

3.3.1. Effect of Ionization Method. Petroleomic is a very powerful approach to illustrate thousands of molecular components in various graphical representations. To conduct the analysis of complex mixtures, the majority of the compounds has to be efficiently ionized and detected. The ionization step must generate molecular or pseudomolecular ions as, for example, protonated or deprotonated species and avoid fragmentation phenomenon, which significantly complicates the interpretation of the obtained data.

The main limitation of the petroleomic approach is the difference in ionization yields between compounds. The ionization technique has to be sensitive and yield comparable ionization rates for all classes of compounds present in the investigated sample to limit discrimination or ionization competition. Unfortunately, real world complex mixture often does not adopt this ideal behavior due to significant chemical property differences of the components. As a consequence, it was chosen in this study to use two complementary ionization techniques. The first one is ESI, which is known to be one of the softest ionization techniques coupled to mass spectrometry. Nevertheless, the ESI is only poorly efficient for nonpolar or less polar chemicals. To overcome this problem, an alternative and complementary ionization technique was used. The LDI method is known to efficiently ionized compounds, which present a significant absorption at the wavelength of the used laser. The species have to be highly unsaturated and/or include a significant number of heteroatoms. It is expected that their absorption coefficient at the laser wavelength (355 nm, in this case) is high enough to efficiently induce the desorption and the ionization phenomena and to decrease the laser power density to avoid fragmentation processes. This approach has been used for the analysis of environmental, materials science, or petroleum.[52−56]

The HDO reactions significantly modify the functional groups; for example, hydroxyl or methoxy functions are replaced by hydrogen atom and polarity is reduced. Consequently, the study of the selectivity of HDO processes requires different ionization methods such as negative LDI and ESI. Mass spectra for lignin pyrolysis (no catalyst, empty second reactor at 400 °C) obtained by LDI and ESI are presented in Figure 5.

A large number of peaks are detected, close to 300 peaks by ESI FT ICR MS and more than 600 peaks by LDI FT ICR MS.

dx.doi.org/10.1021/ef302145g | *Energy Fuels* 2013, 27, 2135−2145

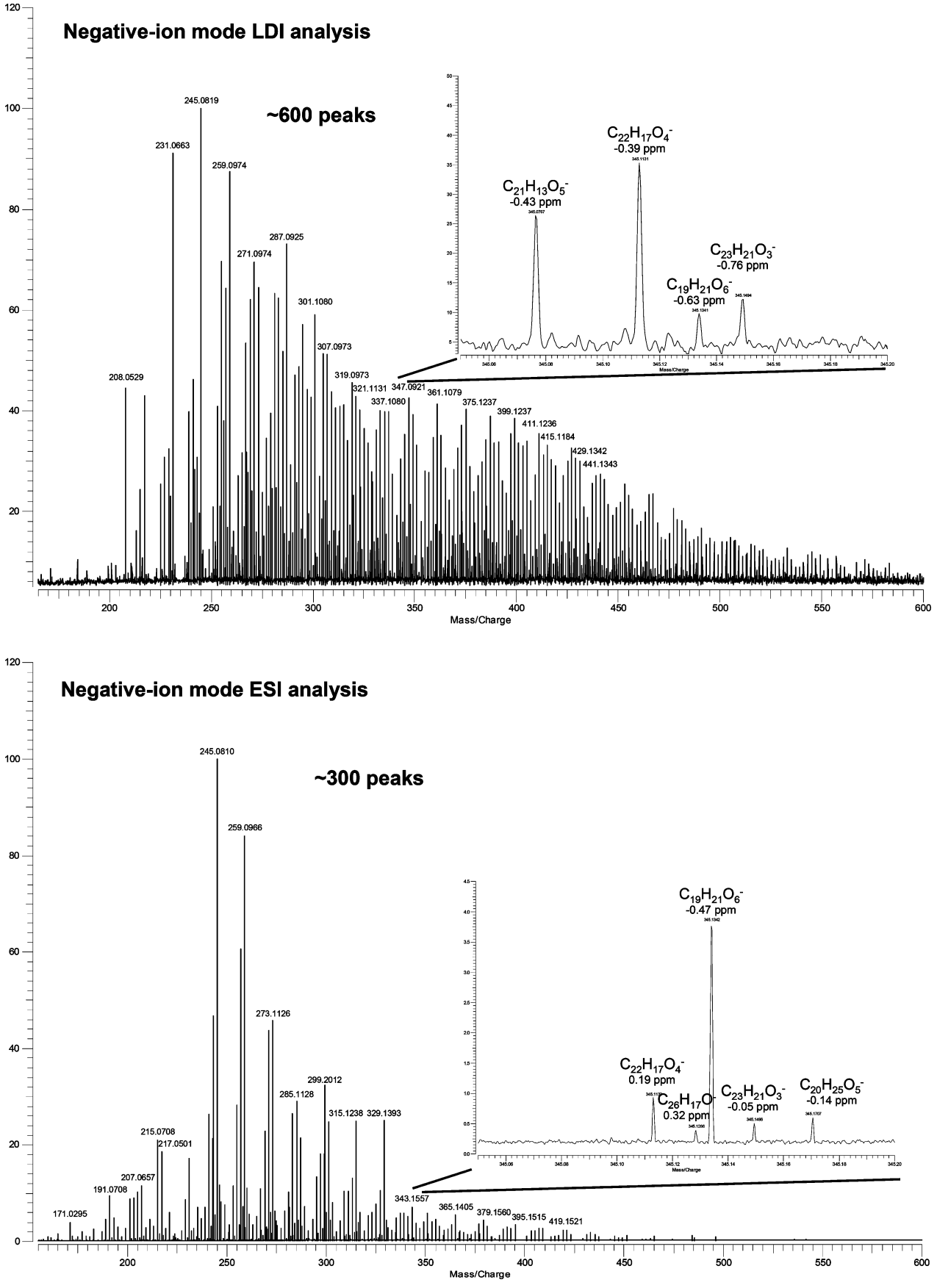

Figure 5. Mass spectra of methanol-soluble species from lignin pyrolysis (empty second reactor set at 400 °C) by LDI and ESI both in negative-ion mode, with a zoom emphasizing complementarity between LDI and ESI. These spectra correspond to the same sample as analyzed in Figures 2 and 4a by GC.

dx.doi.org/10.1021/ef302145g | *Energy Fuels* 2013, 27, 2135−2145

The main contributions are relative to $C_xH_yO_z$ species. The list of peaks detected by LDI is given in the Supporting Information.

In ESI mode, deprotonated species are specifically observed, whereas radical cations are also observed by LDI mode.

Different processes are responsible for the ions formation in LDI. The first is relative to the photoionization phenomenon and corresponds to the release of an electron from the investigated compound upon laser irradiation and the production of radical cation $M^{\bullet+}$, which may be observed in positive ion detection mode (results not shown). The molecule is first desorbed because such a process only occurs in the gas phase. The released electron may interact with species in the gas phase and yield radical anion $M^{\bullet-}$ by electron capture if the electron affinity of the compound is high enough and the generated electrons cold enough. Alternatively, the release of protons in the gas phase to form $[M - H]^-$ ions from different compounds ensures to increase the amount of H^+ in the gas phase. Molecules with high gas-phase proton affinity may then be ionized by proton capture and detected in positive detection mode (not shown).

Proton transfer phenomenon is the key parameter to rationalize the nature of the species detected by ESI. The acid/base properties of the oxygen-containing compounds from the lignin-derived products enable their efficient ionization by ESI, as was previously shown.[27−29,45] Hydroxyl functional groups can be easily deprotonated and yield negative ion ESI.[27,28,45]

The m/z ranges of detected ions are influenced by the used ionization method. The ESI mass spectrum displays anions in the 170−450 m/z range, whereas LDI yields ions in a much broader range, between m/z 200 and 650 (Figure 5). It can be mainly explained by different ionization efficiency but also by different ions transfer efficiency. Even if the instrument parameters were optimized to transfer the ions in the same m/z range, the RF amplitude (275 $V_{b\text{-}p}$) and the RF frequency (1.965 MHz) of the ESI card are a little bit higher than those of the LDI one (200 $V_{b\text{-}p}$ and 1.840 MHz). Nevertheless, a modification of the instrument parameters to favor the transfer of heavier ions in ESI did not lead to a modification of the mass spectrum at high m/z ratio. Consequently, the ionization efficiency seems to be the most critical parameter to explain the differences between LDI and ESI.

Figure 6 displays the distribution in oxygen content class and double bond equivalent (DBE)[57] for LDI and ESI analysis. For a molecule with an elemental formula $C_cH_hN_nO_oS_s$, the DBE is calculated by the following relation:

$$\mathrm{DBE} = c - \frac{h}{2} + \frac{n}{2} + 1$$

The DBE reflects the "unsaturation degree" of molecules. It is higher for unsaturated molecules (more condensed, aromatics) with a lower H/C ratio.

According to Figure 6, the DBE of the detected species is definitely higher for compounds ionized by LDI. Moreover, Figure 6 also shows that LDI detected ions are more oxygenated. Our results are consistent with the study of Smith et al.[26] who showed a distribution in oxygen class compound between O_4 and O_8 by LDI for lignin pyrolysis products.[27] It clearly evidenced that higher m/z peaks are associated with more unsaturated and oxygenated compounds, which are more efficiently ionized by LDI (vs ESI).

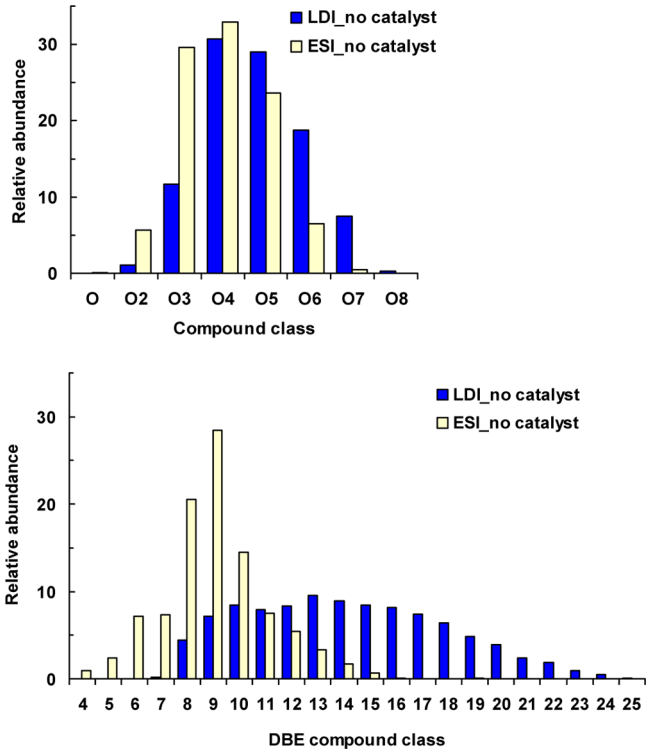

Figure 6. Oxygen and DBE class analysis for lignin pyrolysis products (no catalyst in the second reactor at 400 °C) for negative-ion mode LDI and ESI analysis.

In ESI mode, the detected species are more saturated and contained a more restricted number of oxygen (between O_2 and O_6, Figure 6). Their significant abundance could be related to a more polar behavior, which may be tentatively assigned to hydroxyl groups with a labile hydrogen atom, promoting the deprotonation process to yield $[M - H]^-$ anions. Moreover, these species (low mass and restricted number of oxygen atoms) are more volatile. Part of them could be vaporized inside the LDI source vacuum (10^{-2}−10^{-4} Torr) before the data acquisition and cannot be observed in the LDI mass spectrum.

To sum, ESI and LDI have to be seen as complementary ionization techniques, which reveal different class of components: a highly polar one in ESI and less polar, more conjugated, heavier, and on a broader range of m/z in LDI. The ability of LDI to efficiently ionize such components has been previously demonstrated.[26,52−56]

Figure 7 displays the modified Van Krevelen diagram of LDI and ESI for lignin pyrolysis products (without catalyst).[58]

The lignin pyrolysis products (without catalyst) are still mainly oxygenated (with OH groups),[13] and ESI would be adapted to ionize them efficiently. Nevertheless, LDI ionizes a much broader range of species and with the major products at higher O/C and H/C (vs ESI). Dimers and trimers of lignin are well analyzed by LDI in agreement with Smith et al.[26] and Bayerbach and Meier.[13] The Van Krevelen distribution obtained by LDI is very close to the distribution observed for GC-oils (Figure 4a). These heavy lignin oligomers would exhibit about the same elemental composition distribution as the monomers analyzed by GC (such as catechol, guiacol, Figure 4a). In an extensive work on the analysis of pyrolytic lignin, Meier et al.[10,13] revealed some molecular structures of dimers and trimers by LDI TOF MS and pyrolysis-GC/MS

dx.doi.org/10.1021/ef302145g | Energy Fuels 2013, 27, 2135−2145

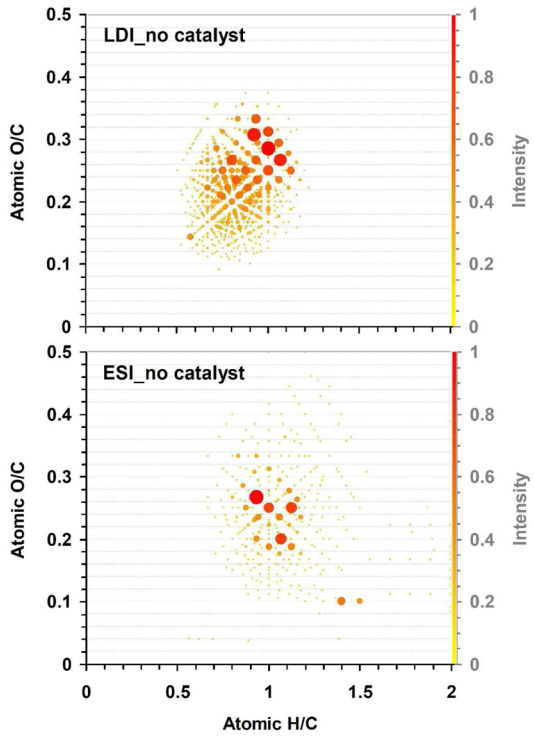

Figure 7. Van Krevelen diagram of lignin pyrolysis without catalyst (empty second reactor at 400 °C) for LDI and ESI (MS spectra presented in fFgure 5). These diagrams correspond to the same sample as in Figure 4a analyzed by GC. The area and color of each circle are a function of the relative intensity (and not the weight yield) of each corresponding molecule.

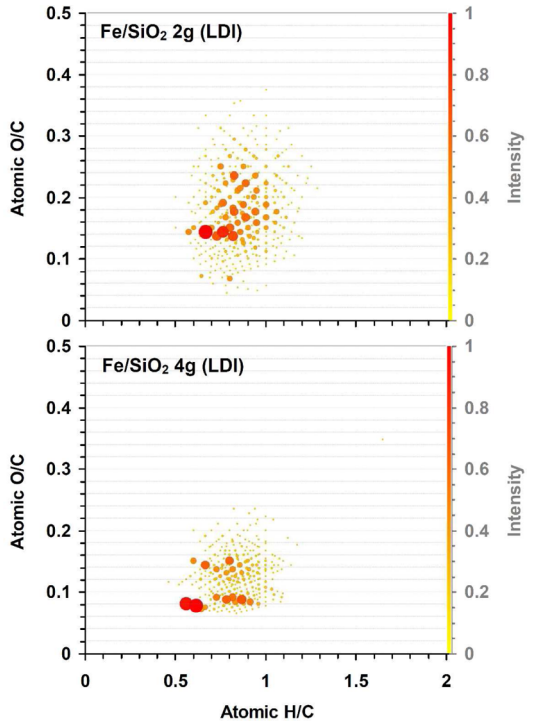

Figure 8. Van Krevelen diagram obtained by LDI FT ICR MS analysis of lignin pyrolysis products as a function of the mass of Fe/SiO_2 catalyst. Pyrolysis and catalytic fixed bed reactors set at 500 and 400 °C, respectively, for both conditions. These spectra correspond to the same sample as in Figure 4b,c analyzed by GC. The area and color of each circle represent the relative intensity of each corresponding molecule.

(among other techniques). Some major species, for instance, at 272, 302, and 386 Da, are analyzed in both of our studies. Smith et al.[26] also revealed the compounds at 272, 284, 298, and 310 Da. Nevertheless, it is difficult to compare our results with other works because the composition of pyrolysis products depends on the pyrolysis conditions and on the chemical structure of lignin, which, in turn, depends on the original biomass and the extraction procedure.[59] The analysis by MS/MS of the chemical structural of the molecules is out of the scope of this Article.

The different ionization selectivity between LDI and ESI is even more marked on hydrotreated products (ESI analysis of 4 g of Fe/SiO_2 given in the Supporting Information). ESI is more specific to polar compounds and enhances them. LDI efficiently ionizes again a broader range of species than ESI, and Van Krevelen distribution (Figure 8) is more consistent with GC analysis (Figure 4b,c). LDI is clearly adapted to detect our hydrodeoxygenated products (more unsaturated and less protic). ESI is yet a method of choice for sugaric species from holocelluloses primary pyrolysis[27−29] and to reveal polar species refractory to the hydrotreatment.

3.3.2. Effect of Catalytic Treatment on Distribution of Species Analyzed by Petroleomic. Figure 8 depicts the Van Krevelen diagrams obtained by LDI as a function of the mass of Fe/SiO_2 catalyst.

Petroleomic analysis on Fe/AC catalyst showed a very weak signal highlighting a much lower content in heavier species as compared to Fe/SiO_2. It is consistent with the finding that Fe/AC produces a more transparent solution than Fe/SiO_2 (see the picture of solutions in the Supporting Information). This feature could be attributed to different surface chemistry between activated carbon and silica but also to different porous structure. Indeed, activated carbon is microporous, whereas silica is mesoporous.

The H/C and O/C distributions of heavier products analyzed by LDI FT ICR MS are lower and higher, respectively, than GC-oils and for the two Fe/SiO_2 masses (Figure 4b,c). Heavier products are more condensed (unsaturated) as compared to lighter ones and most probably less efficiently hydrodeoxygenated by the catalyst. The heavier species produced by lignin pyrolysis are probably more reactive than lighter ones (analyzed by GC) and more strongly adsorbed on the catalysts. The hydrotreatment would be less selective for heavier species because the cracking and growth (decrease in H/C) would be promoted as compared to the HDO (C−O cleavage and stabilization with spilt-over H-species). This mechanism is consistent with our previous discussion on the mechanism on coke formation from guaiacol HDO.[42]

Nevertheless, on the basis of the Van Krevelen diagrams (Figure 8), it is very clear that Fe/SiO_2 deoxygenates these heavier products although less selectively than the GC-oils. Unfortunately, heavy species produced without and with the catalyst cannot be quantified by petroleomic. One has to keep in mind that the mass yield between each experiment can be very different especially when lignin pyrolysis (without catalyst) and catalytic treatment are compared. Only relative distributions in species can be compared for different experiment conditions.

Figure 9 displays the relative abundance of oxygen class compounds as a function of the catalytic treatment.

dx.doi.org/10.1021/ef302145g | *Energy Fuels* 2013, 27, 2135−2145

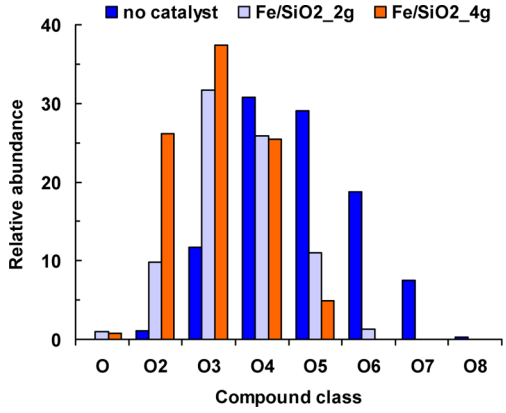

Figure 9. Distribution in oxygen class analyzed by LDI FT ICR MS as a function of the catalytic treatment.

Very oxygenated species (from O_6 to O_8) from lignin pyrolysis are no more produced after the catalytic treatment (Figure 9). A progressive increase (in terms of relative abundance) in O_2 and O_3 species combined with a decrease in O_4 and O_5 compounds is evidenced when the mass of Fe/SiO_2 increases. This tendency is also partially observed with ESI analysis, but it is definitely less significant than for LDI analysis. Indeed, the partition of the ionization in ESI impedes the detection of the low oxygenated compounds and alters the analyzed distribution of species. Heavy species are most probably deposited over the catalyst, interact strongly with the support, and further react. To the best of our knowledge, we give the first results on the evolution of the heavy products (>300 Da) of bio-oils during their catalytic treatment. It would be of great interest in future works to combine petroleomic analysis with quantitative analysis (such as LC/MS) and catalysts characterizations.

4. DISCUSSION ON THE COMPLEMENTARITY BETWEEN GC AND PETROLEOMIC ANALYSIS

Van Krevelen diagrams are very meaningful to illustrate the evolution in H/C and O/C ratios of hundreds of species, but they do not depict the evolution of the molecular weights. The selectivity of catalytic processes cannot therefore be solely assessed by such charts.

To highlight the high complementarity between GC and petroleomic analysis, carbon and oxygen numbers of species analyzed by these two methods are plotted in Figure 10 as a function of their weight yield for GC analysis and relative abundance for petroleomic. The area of circles cannot be compared between each analytical method but just between experimental conditions for the same analytical method.

A much broader range of species is analyzed by petroleomic, from O_2 to O_8 and C_8 to C_{37} in lignin products (without catalyst, Figure 10), whereas species up to O_4 and C_{14} are analyzed by GC. It is important to notice the effect of the catalytic treatment on the distribution of species. Some zones of interest are brought out in Figure 10.

During the catalytic treatment, GC-oils (in red in Figure 10) are deoxygenated without an increase in the carbon number (little growth). Light species, such as acetic acid at C_2 and O_2, are converted by the catalytic treatment. O_2 class molecules are almost completely converted in O_1 and O_0 species, but their DBE does not increase (not shown). The alkylation is well depicted by this chart (increase in C_8 species). Deoxygenation

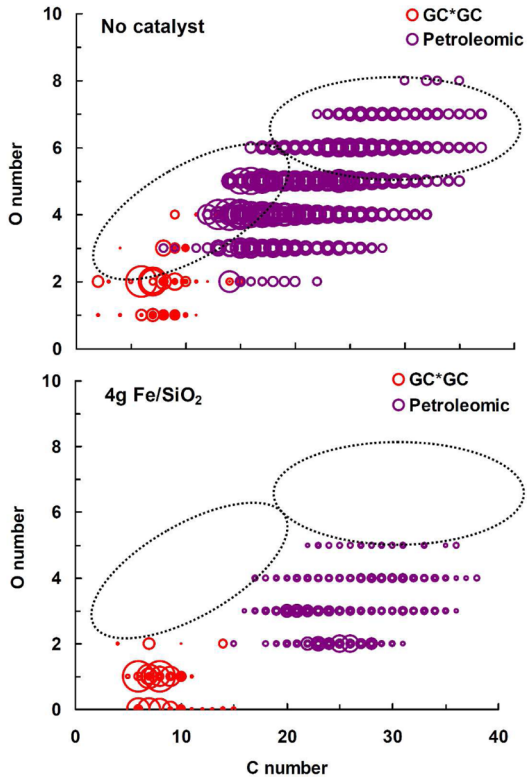

Figure 10. Compound class (C and O numbers) determined by GC*GC and petroleomic analysis (LDI) as a function of weight yield for GC and relative abundance for petroleomic, for lignin pyrolysis without catalyst, and 4 g of Fe/SiO_2 treatment. The area of circles is a function of weight yield for species analyzed by GC and relative abundance for petroleomic and cannot be compared between the two analytical methods. It can be compared only between the two experimental conditions and for the same analytical method.

and alkylation reactions are thus achieved without condensation of the C_6–C_8 species.

Concerning the petroleomic analysis, Figure 10 shows that the main species are O_4–O_5 and C_{13}–C_{20} for lignin pyrolysis (without catalyst) but after the catalytic treatment heavy species are less oxygenated (mainly O_2 and O_3 classes) but with higher carbon number classes (C_{20} to C_{30}) and with a higher DBE (not shown). Heavier lignin oligomers are more prone to growth and condensation than monoaromatic species analyzed by GC. The heaviest species (with more than 5 oxygen atoms) are completely trapped or converted by the catalytic bed (zone highlighted in Figure 10).

The heavy species are most probably poorly converted into GC-oils; otherwise, the weight yields in GC-oils would have increased instead of decreasing after the catalytic treatment. They are mainly converted into coke deposit (not investigated in this Article).

The main challenge for the HDO of lignin pyrolysis products, and also for biomass pyrolysis,[12] is to convert the heavy lignin oligomers into fuels or valuable aromatics such as BTX or phenol. New catalytic systems have still to be looked for.

5. CONCLUSION

To the best of our knowledge, this Article presents the first quantitative GC*GC analysis (by the so-called "heart-cutting" method) combined with very high-resolution mass spectrom-

dx.doi.org/10.1021/ef302145g | Energy Fuels 2013, 27, 2135–2145

etry analysis ("petroleomic" method) applied to the hydrotreatment of lignin-derived pyrolysis oils. These two analytical methods are very complementary and are needed to assess the selectivity of the catalytic treatments both for light (GC-analyzable) and for heavier species (analyzed by petroleomic). Modified Van Krevelen diagrams depict "maps" that are relevant chemical signatures of bio-oils. The distributions of species as a function of O and C numbers are charts complementary to Van Krevelen diagrams. This analytical methodology could help to highlight new catalytic mechanisms and to design new catalytic reactors.

■ ASSOCIATED CONTENT

Supporting Information

Experimental setup for pyrolysis and catalytic conversion of vapors, the calibration method for the GC*GC/FID heart-cutting analysis, a complete list of all species quantified by GC*GC, a complete list of all species detected by petroleomic analysis, Van Krevelen diagram of negative-mode ESI FT ICR MS analysis of hydrotreated bio-oils, and a picture of the analyzed solutions (bio-oils + methanol) after different catalytic treatments. This material is available free of charge via the Internet at http://pubs.acs.org.

■ AUTHOR INFORMATION

Corresponding Author

*E-mail: anthony.dufour@univ-lorraine.fr.

Notes

The authors declare no competing financial interest.

■ ACKNOWLEDGMENTS

The very big infrastructure program of CNRS ("TGIR" program) is acknowledged for some financial support. Prof. D. Meier from the Institute of Wood Chemistry (Hamburg, Germany) is acknowledged for supplying the lignin sample. G. Lardier and Michel Mercy (CNRS, Nancy) are also thanked for their technical help in conducting the pyrolysis experiments.

■ REFERENCES

(1) Huber, A.; Corma, A. *Angew. Chem., Int. Ed.* **2007**, *46*, 7184−7201.
(2) Bridgwater, A. V. *Biomass Bioenergy* **2012**, *38*, 68−94.
(3) Valle, B.; Castaño, P.; Olazar, M.; Bilbao, J.; Gayubo, A. G. *J. Catal.* **2012**, *285*, 304−314.
(4) Elliott, D. C.; Hart, T. R.; Neuenschwander, G. G.; Rotness, L. J.; Zacher, A. H. *Environ. Prog. Sustainable Energy* **2009**, *28*, 441−449.
(5) Oasmaa, A.; Meier, D. *J. Anal. Appl. Pyrolysis* **2005**, *73*, 323−334.
(6) Oasmaa, A.; Kuoppala, E.; Elliott, D. C. *Energy Fuels* **2012**, *26*, 2454−2460.
(7) Garcia-Perez, M.; Chaala, A.; Pakdel, H.; Kretschmer, D.; Roy, C. *Biomass Bioenergy* **2007**, *31*, 222−242.
(8) Gellerstedt, G.; Li, J.; Eide, I.; Kleinert, M.; Barth, T. *Energy Fuels* **2008**, *22*, 4240−4244.
(9) Hoekstra, E.; Kersten, S. R. A.; Tudos, A.; Meier, D.; Hogendoorn, K. J. A. *J. Anal. Appl. Pyrolysis* **2011**, *91*, 76−88.
(10) Scholze, B.; Meier, D. *J. Anal. Appl. Pyrolysis* **2001**, *60*, 41−54.
(11) Branca, C.; Giudicianni, P.; Di Blasi, C. *Ind. Eng. Chem. Res.* **2003**, *42*, 3190−3202.
(12) Garcia-Perez, M.; Wang, S.; Shen, J.; Rhodes, M.; Lee, W. J.; Li, C.-Z. *Energy Fuels* **2008**, *22*, 2022−2032.
(13) Bayerbach, R.; Nguyen, V. D.; Schurr, U.; Meier, D. *J. Anal. Appl. Pyrolysis* **2006**, *77*, 95−101.
(14) Xu, F.; Xu, Y.; Yin, H.; Zhu, X.; Guo, Q. *Energy Fuels* **2009**, *23*, 1775−1777.
(15) Fratini, E.; Bonini, M.; Oasmaa, A.; Solantausta, Y.; Teixeira, J.; Baglioni, P. *Langmuir* **2006**, *22*, 306−312.
(16) Dilcio Rocha, J.; Luengo, C. A.; Snape, C. E. *Org. Geochem.* **1999**, *30*, 1527−1534.
(17) Mullen, C. A.; Strahan, G. D.; Boateng, A. A. *Energy Fuels* **2009**, *23*, 2707−2718.
(18) Marshall, A. G.; Hendrickson, C. L.; Jackson, G. S. *Mass Spectrom. Rev.* **1998**, *17*, 1−35.
(19) Marshall, A. G.; Rodgers, R. P. *Acc. Chem. Res.* **2004**, *37*, 53−59.
(20) Marshall, A. G.; Rodgers, R. P. *Proc. Natl. Acad. Sci. U.S.A.* **2008**, *105*, 18090−18095.
(21) Klein, G. C.; Kim, S.; Rodgers, R. P.; Marshall, A. G.; Yen, A. *Energy Fuels* **2006**, *20*, 1973−1979.
(22) Gaspar, A.; Zellermann, E.; Lababidi, S.; Reece, J.; Schrader, W. *Energy Fuels* **2012**, *26*, 3481−3487.
(23) Miyabayashi, K.; Naito, Y.; Miyake, M. *J. Jpn. Pet. Inst.* **2009**, *52*, 159−171.
(24) Hughey, C. A.; Hendrickson, C. L.; Rodgers, R. P.; Marshall, A. G. *Energy Fuels* **2011**, *15*, 1186−1193.
(25) Omais, B.; Charon, N.; Courtiade, M.; Ponthus, J.; Thiébaut, D. *Fuel* **2013**, *104*, 805−812.
(26) Smith, E. A.; Lee, Y. J. *Energy Fuels* **2010**, *24*, 5190−5198.
(27) Smith, E. A.; Park, S.; Klein, A. T.; Lee, Y. J. *Energy Fuels* **2012**, *26*, 3796−3802.
(28) Jarvis, J. M.; McKenna, A. M.; Hilten, R. N.; Das, K. C.; Rodgers, R. P.; Marshall, A. G. *Energy Fuels* **2012**, *26*, 3810−3815.
(29) Liu, Y.; Shi, Q.; Zhang, Y.; He, Y.; Chung, K. H.; Zhao, S.; Xu, C. *Energy Fuels* **2012**, *26*, 4532−4539.
(30) Amundson, L. M.; Gallardo, V. A.; Vinueza, N. R.; Owen, B. C.; Reece, J. N.; Habicht, S. C.; Fu, M.; Shea, R. C.; Mossman, A. B.; Kenttämaa, H. I. *Energy Fuels* **2012**, *26*, 2975−2989.
(31) Barbier, J.; Charon, N.; Dupassieux, N.; Loppinet-Serani, A.; Mahé, L.; Ponthus, J.; Courtiade, M.; Ducrozet, A.; Quoineaud, A.-A.; Cansell, F. *Biomass Bioenergy* **2012**, *46*, 479−491.
(32) Zhong, J.; Sleighter, R. L.; Salmon, E.; McKee, G. A.; Hatcher, P. G. *Org. Geochem.* **2011**, *42*, 903−916.
(33) Grinhut, T.; Hertkorn, N.; Schmitt-Kopplin, P.; Hadar, Y.; Chen, Y. *Environ. Sci. Technol.* **2011**, *45*, 2748−2754.
(34) Dutriez, T.; Courtiade, M.; Ponthus, J.; Thiébaut, D.; Dulot, H.; Hennion, M.-C. *Fuel* **2012**, *96*, 108−119.
(35) Fogassy, G.; Lorentz, C.; Toussaint, G.; Thegarid, N.; Schuurman, Y.; Mirodatos, C. *Environ. Prog. Sustainable Energy* **2012**, in press, DOI: 10.1002/ep.10631.
(36) Rodgers, R. P.; White, F. M.; Hendrickson, C. L.; Marshall, A. G.; Andersen, K. V. *Anal. Chem.* **1998**, *70*, 4743−4750.
(37) Wu, Z.; Rodgers, R. P.; Marshall, A. G.; Strohm, J. J.; Song, C. *Energy Fuels* **2005**, *19*, 1072−1077.
(38) Kekäläinen, T.; Pakarinen, J. M. H.; Wickström, K.; Vainiotalo, P. *Energy Fuels* **2009**, *23*, 6055−6061.
(39) Miyabayashi, K.; Naito, Y.; Yamada, M.; Miyake, M.; Ushio, M.; Fuchigami, J.; Kuroda, R.; Ida, T.; Hayashida, K.; Ishihara, H. *Fuel Process. Technol.* **2008**, *89*, 397−405.
(40) Stihle, J.; Uzio, D.; Lorentz, C.; Charon, N.; Ponthus, J.; Geantet, C. *Fuel* **2012**, *95*, 79−87.
(41) Jarvis, J. M.; McKenna, A. M.; Hilten, R. N.; Das, K. C.; Rodgers, R. P.; Marshall, A. G. Proceeding of the ASMS conference, Vancouver, 2011.
(42) Olcese, R. N.; Bettahar, M.; Petitjean, D.; Malaman, B.; Giovanella, F.; Dufour, A. *Appl. Catal., B: Environ.* **2012**, *115*−*116*, 63−73.
(43) Olcese, R.; Bettahar, M. M.; Malaman, B.; Ghanbaja, J.; Tibavizco, L.; Petitjean, D.; Dufour, A. *Appl. Catal., B: Environ.* **2013**, *129*, 528−538.
(44) Dufour, A.; Girods, P.; Masson, E.; Normand, S.; Rogaume, Y.; Zoulalian, A. *J. Chromatogr., A* **2007**, *1164*, 240−247.
(45) Amundson, L. M.; Eismin, R. J.; Reece, J. N.; Fu, M.; Habicht, S. C.; Mossman, A. B.; Shea, R. C.; Kenttämaa, H. I. *Energy Fuels* **2011**, *25*, 3212−3222.

(46) de Saint Laumer, J.-Y.; Cicchetti, E.; Merle, P.; Egger, J.; Chaintreau, A. *Anal. Chem.* **2010**, *15*, 6457−6462.
(47) McIver, R. T. *Int. J. Mass Spectrom.* **1990**, *98*, 35−50.
(48) De Wild, P.; Van Der Laan, R.; Kloekhorst, A.; Heeres, E. *Environ. Prog. Sustainable Energy* **2009**, *28*, 461−469.
(49) van Krevelen, D. W. *Fuel* **1950**, *29*, 269−284.
(50) Johnson, D.; Chornet, E.; Zmierczak, W.; Shabtai, J. *Prepr. Pap.-Am. Chem. Soc., Div. Fuel Chem.* **2002**, 380.
(51) Popov, A.; Kondratieva, E.; Goupil, J. M.; Mariey, L.; Bazin, P.; Gilson, J.-P.; Travert, A.; Maugé, F. *J. Phys. Chem. C* **2010**, *114*, 15661−15670.
(52) Schramm, S.; Carré, V.; Scheffler, J.-L.; Aubriet, F. *Anal. Chem.* **2011**, *83*, 133−142.
(53) Carré, V.; Aubriet, F.; Scheepers, P. T.; Krier, G.; Muller, J.-F. *Rapid Commun. Mass Spectrom.* **2005**, *19*, 871−880.
(54) Aubriet, F.; Carré, V. *Anal. Chim. Acta* **2010**, *659*, 34−54.
(55) Cho, Y.; Witt, M.; Kim, Y. H.; Kim, S. *Anal. Chem.* **2012**, *84*, 8587−8594.
(56) Cho, Y.; Jin, Y. M.; Witt, M.; Birdwell, J. E.; Na, J.-G.; Roh, N.-S.; Kim, S. *Energy Fuels*, DOI: 10.1021/ef3015662.
(57) Vetter, W.; McLafferty, F. W.; Turecek, F. *Interpretation of Mass Spectra*, 4th ed.; University Science Books: Mill Valley, CA, 1993.
(58) Kim, S.; Kramer, R. W.; Hatcher, P. G. *Anal. Chem.* **2003**, *75*, 5336−5344.
(59) Jakab, E.; Faix, O.; Till, F.; Székely, T. *J. Anal. Appl. Pyrolysis* **1995**, *35*, 167−179.